Fuzzy ARTMAP classification of invariant features derived using angle of rotation from a neural network

P. Raveendran [a,*], R. Palaniappan [a], Sigeru Omatu [b]

[a] *Department of Electrical and Telecommunication, Engineering Faculty, University of Malaya, Kuala Lumpur 50603, Malaysia*
[b] *Department of Computer and System Science, College of Engineering, University of Osaka Perfecture, Sakai, Osaka 593, Japan*

Abstract

Conventional regular moment functions have been proposed as pattern sensitive features in image classification and recognition applications. But conventional regular moments are only invariant to translation, rotation and equal scaling. It is shown that the conventional regular moment invariants remain no longer invariant when the image is scaled unequally in the x- and y-axis directions. We address this problem by presenting a technique to make the regular moment functions invariant to unequal scaling. However, the technique produces a set of features that are only invariant to translation, unequal/equal scaling and reflection. They are not invariant to rotation. To make them invariant to rotation, moments are calculated with respect to the principal axis of the image. To perform this, the exact angle of rotation must be known. But the method of using the second-order moments to determine this angle will also be inclusive of an undesired tilt angle. Therefore, in order to correctly determine the amount of rotation, the tilt angle which differs for different scaling factors in the x- and y-axis directions for the particular image must be obtained. In order to solve this problem, a neural network using the back-propagation learning algorithm is trained to estimate the tilt angle of the image and from this the amount of rotation for the image can be determined. Next, the new moments are derived and a Fuzzy ARTMAP network is used to classify these

---

* Corresponding author. Tel.: +60-379-595-253; fax: +60-377-847-981.
  E-mail address: ravee@fk.um.edu.my (P. Raveendran).

images into their respective classes. Sets of experiments involving images rotated and scaled unequally in the *x*- and *y*-axis directions are carried out to demonstrate the validity of the proposed technique. © 2000 Elsevier Science Inc. All rights reserved.

1. Introduction

High-level image analysis system involves pattern analysis where the automatic recognition of an object in a scene regardless of its position, size and orientation is an important problem. A number of techniques has been developed to derive features from an image, which are invariant under translation, scale change and rotation [1–4]. In particular, the invariant properties of regular moment functions have attracted many users to utilize them as pattern features in object recognition, pattern classification and scene matching [3–9]. Hu [4], in his paper on pattern recognition, derived a set of regular moment invariants based on combinations of regular moments using algebraic invariants. Besides Hu, Bamieh and Figueiredo [12] derived another set of moment invariants using the theory of algebraic invariants. The main characteristic of the invariants formulated by Bamieh and De Figueiredo is that the feature vector size is much lower than any other known invariants, which makes them computationally cheaper. These regular moments are invariant to changes in scale, shift, rotation and reflection.

Hu [4] and Bamieh and Figueiredo [12] have shown that the moments remain invariant when the scale changes in the *x* and *y* directions are equal and the derived features have been used for pattern classification of ship [5] and other applications [6–10]. In some of the applications the scale changes in the *x*- and *y*-axis directions may not be equal. This could be due to the digital nature of the imagery caused by under-sampling and digitizing effects. Or possibly the image itself in comparison with the standard image has unequal scale change in the *x*- and *y*-axis directions. So, when the image is an elongated or compressed version of the original image, as illustrated in Figs. 1(a) and (b), these moments do not remain invariant.
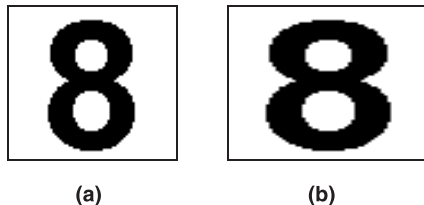

Fig. 1. (a) Original image $f(x, y)$ and (b) unequally scaled and shifted image of (a).

3

We have formed new moments that are invariant to unequal scaling in the *x*- and *y*-axis directions based on the regular moments. However, they are only invariant to scale, translation and reflection. If the scaling constants for the *x*- and *y*-axis directions are equal then rotation invariance can be achieved by combining the moments based on the theory of algebraic invariance as shown in [4]. Rotation invariance can also be achieved by knowing the angle of rotation and using the relationship between the rotated image and its original form to unrotate the image. This angle of rotation is computed by using the principal axis method [11] using the second-order moments. However, this method cannot be used for images that are unequally scaled because the angle of tilt is different if the scale changes in the *x*- and *y*-axis directions are not equal.

So to use the newly derived moments, we have to first achieve invariance to rotation. This can be done if the angle of rotation for the image is determined. However, this angle cannot be determined computationally since the angle obtained using the principal axis method of second-order moments will result in a combination of the rotational angle plus an additional tilt angle which is dependent on the *x*- and *y*-axis scale factors.

As such the tilt angle for the particular image must be known and this is also not possible to be computed since the tilt angle will equal the angle obtained using the principal axis method of second-order moments only if the image is not rotated. As a consequence, when we are dealing with images that are rotated and unequally scaled, an approximating technique has to be considered which will give us the value of the tilt angle. The neural network has been used for this purpose since its parallel architecture and biological structure makes it extremely efficient, especially in those areas where it needs to produce approximations to ill-defined problems [14–18]. For example, Fukumi et al. [17] have used a neural network that consists of two different networks. The first network is intended to learn and recognize standard patterns, whereas the second network comes into play only if the first fails to give a good recognition result. Two different parts use the second network's hidden layer, one part to perform pattern recognition and the other part to perform rotation angle estimation, i.e., it has two properties, rotation-insensitivity and rotation-sensitivity.

In this paper, we have used a more specific approach of using a three-layered neural network trained to estimate the angle of tilt, i.e., the principal axis angle is obtained when the image is not rotated. The input layer of the neural network is presented with six input features of which four of them are second- and third-order moments and the remaining two features are the semimajor and semiminor axis of the image. The back-propagation learning algorithm is used in training the neural network [19]. We have experimented this method with images that are unequally scaled, reflected and rotated. The scaling constants for the *x* and *y* directions are between 0.8 and 1.2 and the images are rotated

through $0°$, $30°$, $60°$, $150°$, $180°$, $225°$ and $300°$. The angle of rotation is computed by subtracting the tilt angle obtained from the neural network with the angle computed from an equation involving second-order moments.

Once the image is obtained in its unrotated form, the new moments can be calculated. Fuzzy ARTMAP [23] is used in classifying these patterns using these newly derived moments. Fuzzy ARTMAP is used instead of other classifiers due to its ability to work with minimal training while maintaining a good classification output and for its quick training.

2. Regular and new moments

The conventional regular moments can be defined as

$$m_{pq} = \int_{-\infty}^{\infty} \int_{-\infty}^{\infty} x^p y^q f(x,y) \, \mathrm{d}x \, \mathrm{d}y \quad \text{for } p, q = 0, 1, 2, \ldots \tag{1}$$

In this paper, we limit ourselves to binary images. For binary images $f(x,y)$ is either 1 or 0. If the region of interest is limited from $(x1, y1)$ to $(x2, y2)$, then we have

$$m_{pq} = \int_{y1}^{y2} \int_{x1}^{x2} x^p y^q f(x,y) \, \mathrm{d}x \, \mathrm{d}y. \tag{2}$$

To make these moments invariants to translation, one can define the central moments as

$$\mu_{pq} = \int_{y1}^{y2} \int_{x1}^{x2} (x - \bar{x})^p (y - \bar{y})^q f(x,y) \, \mathrm{d}x \, \mathrm{d}y, \tag{3}$$

where $\bar{x}$ and $\bar{y}$ are the coordinates of the centroid given by

$$\bar{x} = \frac{m_{10}}{m_{00}}, \qquad \bar{y} = \frac{m_{01}}{m_{00}}. \tag{4}$$

Solving for $\bar{x}$ and $\bar{y}$ and substituting them into (3) gives

$$\mu_{pq} = \int_{y1}^{y2} \int_{x1}^{x2} \left(x - \frac{1}{2}(x_1 + x_2) \right)^p \left(y - \frac{1}{2}(y_1 + y_2) \right)^q f(x,y) \, \mathrm{d}x \, \mathrm{d}y. \tag{5}$$

Using the binomial expansion, (5) can be expressed as

$$\mu_{pq} = \left[\frac{(x_2 - x_1)^{p+1}}{p + 1} + \cdots + C_p^p (x_2 - x_1) \left(-\frac{1}{2}(x_1 + x_2) \right)^p \right]$$
$$\times \left[\frac{(y_2 - y_1)^{q+1}}{q + 1} + \cdots + C_q^q (y_2 - y_1) \left(-\frac{1}{2}(y_1 + y_2) \right)^q \right]. \tag{6}$$

These moments are made invariant to scale change as proposed in [4] by

$$\eta_{pq} = \frac{\mu_{pq}}{\mu_{00}^{(p+q+2)/2}}. \tag{7}$$

Now, consider the unequally scaled image shown in Fig. 1(b). Assume that the expansion in the x and y directions to be α and β, respectively. The central moments can now be defined as

$$\tilde{\mu}_{pq} = \left[\frac{\alpha^{p+1}(x_2 - x_1)^{p+1}}{p+1} + \cdots + C_p^p(x_2 - x_1)\alpha\frac{1}{2}(\alpha\chi_1 + \alpha\chi_2)^p \right]$$
$$\times \left[\beta^{q+1}\frac{(y_2 - y_1)^{q+1}}{q+1} + \cdots + C_q^q(y_2 - y_1)\beta\frac{1}{2}(\beta y_2 + \beta y_1)^q \right]. \tag{8}$$

Evaluating (8) further, the central moments can be expressed in terms of the original moments as

$$\tilde{\mu}_{pq} = \alpha^{p+1}\beta^{q+1}\mu_{pq}. \tag{9}$$

If now (7) is evaluated for the unequally scaled image shown in Fig. 1(b) and expressing in terms of the original image, then we have

$$\tilde{\eta}_{pq} = \left(\frac{\beta}{\alpha} \right)^{(q-p)/2} \eta_{pq}. \tag{10}$$

In order to form moment invariants when $\alpha \neq \beta$, let us consider the following:

$$\lambda_{pq} = \frac{\eta_{pq}}{\eta_{p+1,q+1}} \tag{11}$$

and

$$\tilde{\lambda}_{pq} = \frac{\tilde{\eta}_{pq}}{\tilde{\eta}_{p+1,q+1}}, \tag{12}$$

where once again '$\sim$' refers to moments evaluated for unequally scaled image as shown in Fig. 1(b). Substituting (10) into (12), it is evident that $\tilde{\lambda}_{pq} = \lambda_{pq}$, for $p, q = 0, 1, 2, \ldots$, thereby giving us moment invariance even when $\alpha \neq \beta$.

3. Experimental results for scale invariance and reflection

The images shown in Table 1 are drawn onto a 512×512 grid. An image '4' is considered and the moments for this image are evaluated and tabulated in row 2 of Table 1. Similarly, the moments for unequally scaled and shifted images for various values of and are evaluated. These results are tabulated in rows 3–7 of Table 1. The close agreement obtained in each of these columns

Table 1
New moments for equally and unequally scaled images

Scale	Image	λ_{20}	λ_{02}	λ_{11}	λ_{21}	λ_{12}	λ_{30}	λ_{03}
$\alpha=1.0$ $\beta=1.0$		3.5777	2.2286	1.7794	0.4785	1.1780	2.4226	1.0734
$\alpha=1.0$ $\beta=0.8$		3.5576	2.2220	1.7750	0.4710	1.1742	2.3693	1.0697
$\alpha=1.2$ $\beta=0.8$		3.5957	2.2455	1.7924	0.4733	1.1854	2.3649	1.0807
$\alpha=0.8$ $\beta=1.2$		3.5354	2.1974	1.7562	0.4796	1.1638	2.4704	1.0594
$\alpha=1.2$ $\beta=1.0$		3.6156	2.2523	1.7968	0.4809	1.1892	2.4171	1.0844
$\alpha=1.2$ $\beta=1.2$		3.6289	2.2568	1.7998	0.4859	1.1917	2.4529	1.0869

verifies the correctness of the proposed technique. The reason for not obtaining exact invariance in each column is that the image function is discrete rather than continuous. Since in the foregoing analysis, no assumption was made regarding the values that α or β may assume, we may allow them to become negative. This evidently treats the appropriate mirror reflections and the results are tabulated in Table 2. Once again, the constancy of values obtained in each of the columns demonstrates the validity of the proposed scheme.

4. Rotation property of regular moments

The new regular moments λ_{pq} are invariant under changes of size, translation and reflection but they are not invariant to rotation. In this section, we will discuss the rotational property of the regular moments as a basis for the forthcoming sections. Let us assume that the coordinate origin has been chosen to coincide with the image centroid. The central moments μ_{pq} in the polar form are

Table 2
New moments for reflected images

Images	Reflection	λ_{20}	λ_{02}	λ_{11}	λ_{21}	λ_{12}	λ_{30}	λ_{03}
ⴺ	Original	9.7141	8.5638	1.2819	0.4617	6.6871	7.6125	2.1030
ⴺ	X-axis	9.7141	8.5638	1.2819	0.4617	6.6871	7.6125	2.1030
E	Y-axis	9.7141	8.5638	1.2819	0.4617	6.6871	7.6125	2.1030
E	Both axes	9.7141	8.5638	1.2819	0.4617	6.6871	7.6125	2.1030

$$\mu_{pq} = \int_{-\infty}^{\infty} \int_{-\infty}^{\infty} (r \cos \theta)^p (r \sin \theta)^q f(r,\theta) r \, dr \, d\theta, \tag{13}$$

where $x = r \cos \theta$ and $y = r \sin \theta$ and the Jacobian of the transformation is r.

Now, consider that the image has rotated through an angle ϕ. If the rotated image is denoted by f_r, the relationship between the original and the rotated image in the same polar coordinates is

$$f_r(r,\theta) = f(r, \theta - \phi). \tag{14}$$

By a change of variable $\phi = \theta - \phi$, the moments for the rotated image μ_{pq}^r are

$$\mu_{pq}^r = \int_{-\infty}^{\infty} \int_{-\infty}^{\infty} (r \cos(\phi + \varphi))^p (r \sin(\phi + \varphi))^q r f(r, \varphi) \, dr \, d\varphi. \tag{15}$$

A relationship between the original image μ_{pq} and the rotated image μ_{pq}^r can be established by expanding (15) and expressing it in terms of the moments of the original image. If the image rotates through an angle ϕ, the moments change according to

$$\mu_{pq}^r = \sum_{r=0}^{p} \sum_{s=0}^{q} (-1)^{q-s} \binom{p}{r} \binom{q}{s} (\cos \phi)^{p-r+s} (\sin \phi)^{q+r-s} (\mu_{p+q-r-s, r+s}). \tag{16}$$

The angle of rotation, ϕ, plus the tilt angle, ψ, is determined by using the principle axis method using the second-order moments [11]. The angle $\phi + \psi$ is computed from

$$\phi + \psi = \frac{1}{2} \tan^{-1} \frac{2\mu_{11}}{\mu_{20} - \mu_{02}}. \tag{17}$$

By knowing how much an image has rotated from its original form and by using (18) in the following, only the unequal/equal scaling constants in the x and y directions are left, which can be eliminated by using (11). A neural network is trained to give us the tilt angle, ψ, which can be subtracted from (17) to give us the angle of rotation, ϕ. With this angle and using

$$\mu_{pq}^{ur} = \sum_{r=0}^{p} \sum_{s=0}^{q} (-1)^{p+q-r} \binom{p}{r} \binom{q}{s} (\cos \phi)^{p-r+s} (\sin \phi)^{q+r-s} (\mu_{p+q-r-s,r+s}),$$

$$\tag{18}$$

where μ_{pq}^{ur} is the moment function that is invariant to rotation, we can derive moments for the unrotated image. Using (7) and (11) next will result in a new set of moments that are invariant to translation, rotation and equal/unequal scaling.

5. Rotation angle from neural network

The new moments derived in Section 2 are invariant to translation, reflection and most importantly invariant to scale changes independent of whether it is equal or unequal. But as mentioned, they are not invariant to rotation and an approximation technique has to be developed to ensure that the image is made to be invariant to rotation. The computation of second-order regular moments from (17) gives an angle that consists of the tilt angle, which is inherent in the image and dependent on the scale factors of x- and y-axis and the angle of rotation, if the image is rotated. If the image is not rotated, then the tilt angle will be equal to the computed angle from (17). Fig. 2 shows an image (without
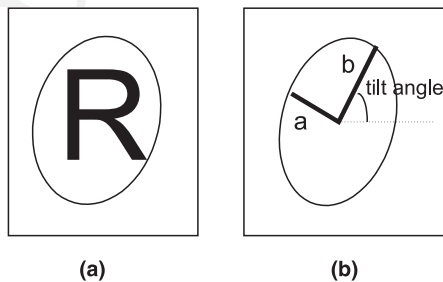

(a)   **(b)**

Fig. 2. (a) An image encircled by an ellipse and (b) semimajor, semiminor and tilt angle of the image in (a).

rotation) encircled by an imaginary ellipse, which serves to better illustrate the concept of the tilt angle.

The problem with rotation arises because the unequal scaling of an image in the x- and y-axis causes the angle of tilt to be different from its original image and also the result obtained by computing the angle using (17) does not indicate if the image is rotated. To solve this problem, a relationship between the standard image and the unequally scaled and rotated image has to be established. A neural network can be used to solve this problem by estimating the tilt angle and from this the amount of rotation for the particular image can be established. Once this is accomplished, the moments for the unrotated image can be obtained where (7) and (11) can be applied to obtain invariance to rotation, translation and equal/unequal scaling.

To measure the tilt angle, a multiplayer perceptron neural network is implemented for this purpose. The neural network, as shown in Fig. 3, is trained to generate the tilt angle of the image in concern. The neural network uses two second-order and two third-order moments as inputs together with another two values of a and b which serve as representations of the semimajor and semiminor axis of the image. The values of a and b are calculated from

$$a = \left[\frac{\mu_{20} + \mu_{02} + \left[(\mu_{20} - \mu_{02})^2 + 4\mu_{11}^2 \right]^{1/2}}{\mu_{00}/2} \right]^{1/2} \quad \text{and}$$

$$b = \left[\frac{\mu_{20} + \mu_{02} - \left[(\mu_{20} - \mu_{02})^2 + 4\mu_{11}^2 \right]^{1/2}}{\mu_{00}/2} \right]^{1/2}. \tag{19}$$
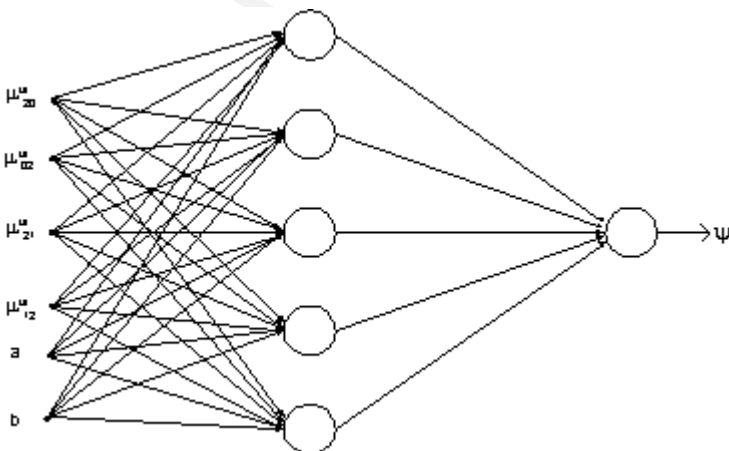

Fig. 3. Neural Network model used to predict tilt angle, ψ.

The target value of each pattern presented to the neural network is the tilt angle and is determined from (17) for an unrotated image. Usage of a and b is needed in reducing the training time of the neural network. This is due to the images that are scaled equally in the x and y directions but different scale factors would produce different second-order moments, however the target (i.e., the tilt angle) would remain the same and this causes confusion for the neural network while training. With the additional values of a and b, which do not change for equal scaling, the neural network converges faster. The back-propagation algorithm is used to train the neural network [19].

Each input is normalised from 0 to 1 to avoid any of them to dominate over the neural network training process. An important fact to note here is that these input features are not invariant to unequal scaling since we need the variance to exist in order to train the neural network to predict the tilt angle, which varies for different unequal scale factors for different images. The output tilt angle is also normalised in the same range to speed up the training process. The predicted tilt angle from the neural network is then renormalized to give us the tilt angle in degrees. The topology of the network is fixed at 6:25:1, i.e., 6 input units, 25 hidden units and a single output unit. The training is conducted until the error in the normalised tilt angle prediction is less than 0.001. The learning rate begins at 0.5 and is reduced with increasing iterations to avoid large oscillations during training. In addition, a momentum value of 0.3 is also used to control the oscillations during training. These parameters were chosen after some preliminary trial runs. Once the output of the net is obtained, the angle of rotation from the x- and y-axis can be determined and hence the image can be obtained in its unrotated form. Next, we can apply the methods discussed in the previous sections to arrive at moments that are invariant to translation, rotation and equal/unequal scaling.

In Section 6, we will discuss Fuzzy ARTMAP [23] network, which is used to classify the images using the newly derived moments to confirm the validity of the proposed method.

6. Fuzzy ARTMAP

ARTMAP is a class of neural network that performs incremental supervised learning of recognition categories in response to input vectors presented in an arbitrary order [20]. Earlier adaptive resonance theory models like ART1 and ART2 consisted of unsupervised learning systems [21,22]. In this paper, a more general ARTMAP system known as Fuzzy ARTMAP is used [23]. This system learns to classify inputs by using fuzzy set features, i.e., the input features are represented by their corresponding membership values from 0 to 1 indicating the extent to which each feature is present. This generalization is accomplished

by replacing the ART1 module of the binary ARTMAP system with Fuzzy ART modules.

Fuzzy ARTMAP incorporates fuzzy set theory in its computation and as such it is able to learn stable responses to either analog or binary valued input patterns. It consists of two Fuzzy ART modules (Fuzzy ART_a and Fuzzy ART_b) that create stable recognition categories in response to sequence of input patterns. During supervised learning, Fuzzy ART_a receives a stream of inputs features representing the pattern and Fuzzy ART_b receives a stream of inputs representing the target class of the pattern. An Inter ART module links these two modules, which is actually an associative controller that creates a minimal linkage of recognition categories between the two Fuzzy ART modules to meet a certain accuracy criterion. This is accomplished by realizing a rule that minimizes predictive error and maximizes predictive generalization. It works by increasing the vigilance parameter ρ_a of Fuzzy ART_a by a minimal amount needed to correct a predictive error at Fuzzy ART_b.

Parameter ρ_a calibrates the minimum confidence that Fuzzy ART_a must have in a recognition category, or hypothesis that is activated by an input vector in order for Fuzzy ART_a to accept that category, rather than search for a better one through an automatically controlled process of hypothesis testing. Lower values of ρ_a enable larger categories to form and lead to a broader generalization and higher code compression. A predictive failure at Fuzzy ART_b increases the minimal confidence ρ_a by the least amount needed to trigger hypothesis testing at Fuzzy ART_a using a mechanism called match tracking. Match tracking sacrifices the minimum amount of generalization necessary to correct the predictive error. Match tracking leads to an increase in the confidence criterion just enough to trigger hypothesis testing which leads to a new selection of Fuzzy ART_a category. This new cluster is better able to predict the correct target class as compared to the cluster before match tracking. Fig. 4(a) shows the general Fuzzy ARTMAP architecture and Fig. 4(b) shows the network structure of Fuzzy ARTMAP as used in this paper. Further details of this method can be found in [20–23].

7. Experimental study

The data set consists of 10 classes of images of numerals 0–9. Each class consists of 25 images that are scaled between 0.8 and 1.2. The basis for this scale factor range is that most unequal scalings of images occur in proximity of the images, for example, as in the case of digitization errors. An example of a class of unequally scaled numeral 2 is shown in Fig. 5 with different scaling constants in the *x*- and *y*-axis directions. Fig. 6 shows an example of numeral 3 that has been rotated with angles of 30°, 60°, 150°, 180°, 225° and 300°. The
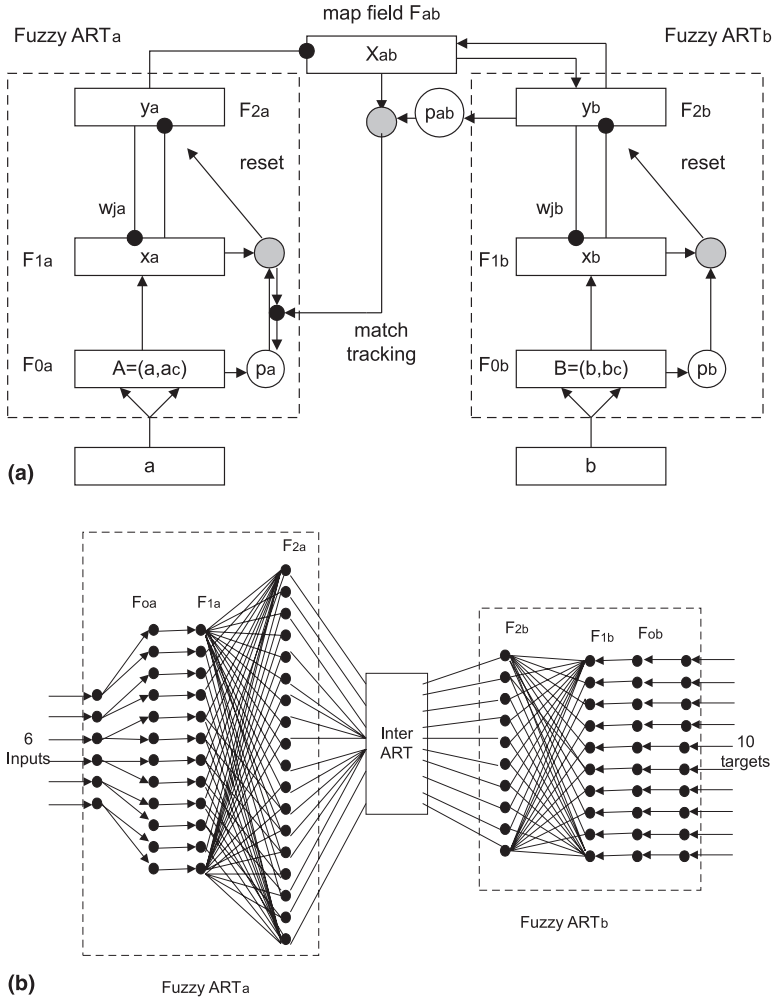
Fig. 4. (a) Fuzzy ARTMAP architecture and (b) Fuzzy ARTMAP showing network structure as used in the experiments in this paper.

total number of images that are rotated and scaled unequally for each class in this experimental study is 175. Therefore, the entire data set consists of 1750 images. Tables 3–5 give the results of the neural network output, i.e., the predicted tilt angle for various cases of scaling factors and rotational angles. The angle of rotation can be obtained from the computed angle minus the predicted angle of tilt from the neural network. The errors for rotational angles 60° and 150° are the same since the neural network's input moment values do

2	2	2	2	2	2	2	2	2
α=1.0β=1.0	α=0.8β=1.1	α=1.2β=1.1	α=1.0β=0.8	α=0.8β=0.9	α=1.2β=0.9	α=1.0β=1.2	α=1.1β=0.8	α=0.9β=1.0
2	2	2	2	2	2	2	2	2
α=1.2β=1.2	α=0.9β=1.1	α=1.1β=1.2	α=0.8β=0.8	α=0.9β=0.9	α=1.2β=0.8	α=1.0β=0.9	α=0.8β=1.0	α=1.2β=1.0
2	2	2	2	2	2	2		
α=1.1β=0.9	α=1.2β=1.0	α=0.8β=1.2	α=0.9β=1.2	α=1.1β=1.0	α=0.9β=0.8	α=1.1β=1.1		

Fig. 5. Numeral 2 with different scaling constants between 0.8 and 1.2.

Fig. 6. Numeral 3 rotated through 0°, 30°, 60°, 150°, 180°, 225° and 300°.

not differ with a 90° difference. As can be seen from the tables, a small error is produced due to lack of enough training for the neural network and also since the images are digital rather than continuous.

Table 3
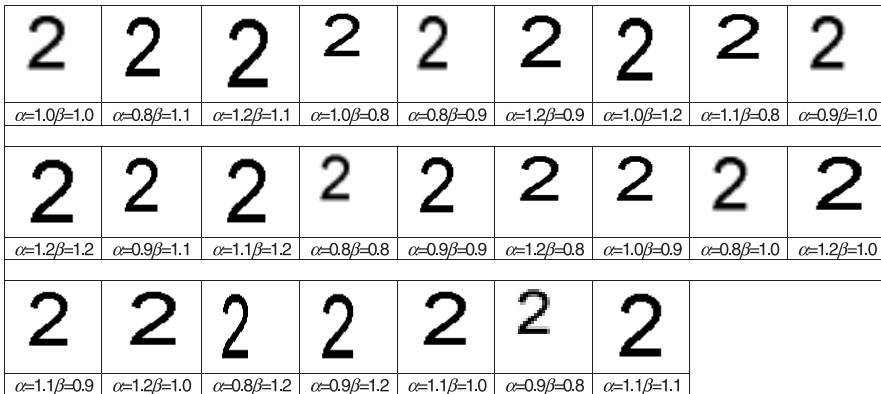Results of images of numeral 2 without rotation

Scaling values		Actual value	Neural Network	Error
$\alpha = 0.8$	$\beta = 0.8$	6.242	6.284	0.042
$\alpha = 0.8$	$\beta = 1.0$	9.802	9.676	0.125
$\alpha = 0.8$	$\beta = 1.2$	16.67	16.42	0.250
$\alpha = 0.9$	$\beta = 0.9$	6.242	6.247	0.005
$\alpha = 0.9$	$\beta = 1.0$	7.587	7.588	0.001
$\alpha = 0.9$	$\beta = 1.1$	9.298	9.202	0.096
$\alpha = 1.0$	$\beta = 0.9$	5.249	5.218	0.031
$\alpha = 1.0$	$\beta = 1.1$	7.438	7.439	0.001
$\alpha = 1.1$	$\beta = 1.0$	5.332	5.291	0.041
$\alpha = 1.1$	$\beta = 1.1$	6.242	6.231	0.011
$\alpha = 1.2$	$\beta = 0.9$	4.027	4.144	0.117
$\alpha = 1.2$	$\beta = 1.1$	5.403	5.387	0.016
$\alpha = 1.2$	$\beta = 1.2$	6.242	6.257	0.015

Table 4
Results for rotated images of numeral 2 with 30°, 60° and 150°

Scaling values		Rotation angle 30°			Rotation angle 60°			Rotation angle 150°		
		Actual value	Neural net	Error	Actual value	Neural net	Error	Actual value	Neural net	Error
$\alpha = 0.8$	$\beta = 0.8$	36.542	6.284	0.250	67.341	6.284	1.057	157.341	6.284	1.057
$\alpha = 0.8$	$\beta = 1.0$	37.709	9.676	1.967	68.176	9.676	1.500	158.176	9.676	1.500
$\alpha = 0.8$	$\beta = 1.2$	45.691	16.42	0.730	73.577	16.42	2.843	163.577	16.42	2.843
$\alpha = 0.9$	$\beta = 0.9$	36.367	6.247	0.120	66.595	6.247	0.348	156.595	6.247	0.348
$\alpha = 0.9$	$\beta = 1.0$	35.864	7.588	1.724	66.125	7.588	1.463	156.125	7.588	1.463
$\alpha = 0.9$	$\beta = 1.1$	37.251	9.202	1.951	70.504	9.202	1.302	160.504	9.202	1.302
$\alpha = 1.0$	$\beta = 0.9$	37.650	5.218	2.432	67.956	5.218	2.738	157.956	5.218	2.738
$\alpha = 1.0$	$\beta = 1.1$	36.988	7.439	0.451	65.071	7.439	2.368	156.071	7.439	2.368
$\alpha = 1.1$	$\beta = 1.0$	36.525	5.291	1.234	66.054	5.291	0.763	156.054	5.291	0.763
$\alpha = 1.1$	$\beta = 1.1$	35.401	6.231	0.830	65.431	6.231	0.800	155.431	6.231	0.800
$\alpha = 1.2$	$\beta = 0.9$	36.605	4.144	2.461	66.616	4.144	2.472	156.616	4.144	2.472
$\alpha = 1.2$	$\beta = 1.1$	37.224	5.387	1.837	67.642	5.387	2.255	157.642	5.387	2.255
$\alpha = 1.2$	$\beta = 1.2$	36.159	6.257	0.098	66.125	6.257	0.132	156.125	6.257	0.132

Table 5
Results for rotated images of numeral 2 with 180°, 225° and 300°

Scaling values		Rotation angle 180°			Rotation angle 225°			Rotation angle 300°		
		Actual value	Neural net	Error	Actual value	Neural net	Error	Actual value	Neural net	Error
$\alpha = 0.8$	$\beta = 0.8$	186.873	6.284	0.589	231.969	6.284	0.685	306.542	6.284	0.258
$\alpha = 0.8$	$\beta = 1.0$	188.574	9.676	1.102	234.768	9.676	0.092	308.709	9.676	0.967
$\alpha = 0.8$	$\beta = 1.2$	193.431	16.42	2.989	240.624	16.42	0.796	313.691	16.42	2.729
$\alpha = 0.9$	$\beta = 0.9$	186.883	6.247	0.636	232.430	6.247	1.183	306.367	6.247	0.120
$\alpha = 0.9$	$\beta = 1.0$	185.975	7.588	1.613	231.577	7.588	1.011	306.864	7.588	0.724
$\alpha = 0.9$	$\beta = 1.1$	187.315	9.202	0.113	234.081	9.202	0.121	309.251	9.202	0.049
$\alpha = 1.0$	$\beta = 0.9$	187.456	5.218	2.238	231.944	5.218	1.726	308.650	5.218	3.432
$\alpha = 1.0$	$\beta = 1.1$	185.423	7.439	2.016	232.926	7.439	0.487	307.988	7.439	0.549
$\alpha = 1.1$	$\beta = 1.0$	186.669	5.291	1.378	231.950	5.291	1.659	306.525	5.291	1.234
$\alpha = 1.1$	$\beta = 1.1$	185.632	6.231	0.599	230.951	6.231	0.280	305.401	6.231	0.830
$\alpha = 1.2$	$\beta = 0.9$	185.580	4.144	1.436	230.644	4.144	1.500	306.605	4.144	2.461
$\alpha = 1.2$	$\beta = 1.1$	187.488	5.387	2.101	232.939	5.387	2.552	307.224	5.387	1.837
$\alpha = 1.2$	$\beta = 1.2$	186.148	6.257	0.109	231.061	6.257	0.196	306.159	6.257	0.098

7.1. Experiment with unequally scaled and rotated images

Next, an experiment is conducted with unequally scaled images combined with rotation. In this experiment, a comparison is made between using a neural network to predict the tilt angle and without using the neural network where a Fuzzy ARTMAP network is used for classification purposes. Both experiments were carried out with the newly derived λ_{pq} moments which consisted of λ_{20}, λ_{02}, λ_{02}, λ_{12}, λ_{30} and λ_{03}. The difference between the two experiments is that the first case uses the angle obtained from (17) (i.e., tilt plus angle of rotation) directly in computing the unrotated moments. Whereas the second case uses a neural network to predict the tilt angle and as such only the angle of rotation is used in computing the unrotated moments after which (7) and (11) are applied to both the cases to obtain λ_{pq}. Therefore, the first case would contain some error. The classification results are as shown in Table 6. All parameters for both the Fuzzy ARTMAP classifications were fixed to be the same and the training data set consisted of a different number of images as shown in the table and the remainder of the images were used for testing. The Fuzzy ART_a vigilance parameter ρ_a is set to 0 since this will allow maximum generalization ability during classification [23].

From Table 6, we can note the increase in classification performance using the newly derived moments, λ_{pq}, for the second case of using a neural network to predict the tilt angle as compared to the case without using the neural network. This shows that using λ_{pq} and a tilt angle prediction from a neural network offers a solution for solving images that are unequally scaled and rotated. A higher classification percentage for the second case can be obtained if the resolution size of the image is increased (i.e., to reduce the digitizing effects) and if the neural network is trained with more patterns to give a more accurate prediction of the tilt angle.

8. Conclusion

The regular moment functions, besides being invariant to translation, rotation and reflection, are only invariant to scale if the scale changes in the *x*-

Table 6
Comparison of Fuzzy ARTMAP classification percentage with and without using a neural network

No. training patterns	Without neural network	With neural network
70	61.24	71.15
140	67.48	74.36
210	72.25	83.15
280	75.35	86.42
350	82.40	94.75

and *y*-axis directions are equal. In this paper, we have proposed new regular moments that are invariant to unequally/equally scaling, translation and reflection. However, they are not invariant to rotation. In order to solve this problem, we have obtained the angle of rotation by using a trained neural network to predict the tilt angle. By using this angle of rotation, invariance to rotation can be achieved and we have shown experimentally that using a set of new equations, moment invariants can be derived for images that are equally/ unequally scaled, translated and rotated.

9. Uncited reference

[13].

References

[1] E. Persoon, K.S. Fu, Shape discrimination using Fourier descriptors, IEEE Transactions on System Man and Cybernatics 7 (1977) 170–179.

[2] Y.N. Hsu, H.H. Arsenault, G. April, Rotational invariant digital pattern recognition using circular harmonic expansion, Applied Optics 21 (1982) 4012–4015.

[3] R.O. Duda, P.E. Hart, Pattern Classification and Scene Analysis, Wiley, New York, 1973.

[4] M.K. Hu, Visual pattern recognition by moment invariants, IRE Transactions on Information Theory 8 (1962) 179–187.

[5] F.W. Smith, M.H. Wright, Automatic ship photo interpretation by the method of moments, IEEE Transactions on Computer 20 (1971) 1089–1094.

[6] S.A Dudani, K.J. Kenneth, R.B. McGhee, Aircraft identification by moment invariants, IEEE Transactions on Computer 26 (1977) 39–45.

[7] S. Reddi, Radial and angular moment invariants for image identification, IEEE Transactions on Pattern Analysis and Machine Intelligence 3 (1981) 240–242.

[8] A. Revees, R. Prokop, S. Andrews, F. Kuhl, Three dimensional shape analysis using moments and Fourier descriptors, IEEE Transactions on Pattern Analysis and Machine Intelligence 10 (1988) 937–943.

[9] P. Raveendran, S. Omatu, Neuro-pattern classification of elongated and contracted images, Information Sciences 3 (1995) 209–221.

[10] A. Khotanzad, J.H. Liu, Classification of invariant image representations using a neural network, IEEE Transactions on Neural Networks 38 (6) (1990) 1028–1038.

[11] M.R. Teague, Image analysis via general theory of moments, Journal of Optical Society of America 70 (1980) 920–930.

[12] R. Bamieh, De Figueiredo, A general moments/attributed-graph method for the three dimensional object recognition from a single image, IEEE Journal of Robotics and Automation 2 (1986) 31–41.

[13] P. Raveendran, S. Omatu, S. Poh, A new technique to derive invariant features for unequally scaled images, in: Proceedings of IEEE International Conference on Systems, Man and Cybernetics, vol. 4, Ocotober 1997, pp. 3158–3163.

[14] P. Raveendran, S. Omatu, S.C. Poh, Using estimation of scaling factor from neural network to derive invariant features, in: Proceedings of IEEE International Conference on Neural Networks, May 1998.

[15] P. Raveendran, S. Omatu, A.B. Wan, Generated moments by neural networks to recognise invariant image representations, Journal of Artificial Neural Networks 1 (3) (1994) 133–147.

[16] M. Fukumi, S. Omatu, F. Takeda, T. Kosaka, Rotation-invariant neural pattern recognition system with application to coin recognition, IEEE Transactions on Neural Networks 2 (3) (1992) 272–279.

[17] M. Fukumi, S. Omatu, Y. Nishikawa, Rotation-invariant neural pattern recognition system estimating a rotation angle, IEEE Transactions on Neural Networks 8 (3) (1997) 568–581.

[18] S.D. You, G.E. Ford, Network model for invariant object recognition and rotation angle estimation, in: Proceedings of International Joint Conference on Neural Networks, vol. 3, 1993, pp. 2145–2148.

[19] D.E. Rumelhart, J.L. McCelland, Parallel Distributed Processing: Exploration in the Microstructure of Cognition, vol. 1, MIT Press, Cambridge, MA, 1986.

[20] G.A. Carpenter, S. Grossberg, J.H. Reynolds, ARTMAP: supervised real time learning and classification of nonstationary data by a self-organising neural network, Neural Networks 4 (1991) 565–588.

[21] G.A. Carpenter, S. Grossberg, A massively parallel architecture for a self-organizing neural pattern recognition machine, Computer Vision, Graphics, and Image Processing 37 (1987) 54–115.

[22] G.A. Carpenter, S. Grossberg, D.B. Rosen, Fuzzy Art: an adaptive resonance algorithm for rapid stable classification of analog patterns, in: Proceedings of International Joint Conference on Neural Networks, vol. 2, pp. 411–420.

[23] G.A. Carpenter, S. Grossberg, N. Markuzon, J.H. Reynolds, D.B. Rosen, Fuzzy ARTMAP: a neural network architecture for incremental supervised learning of analog multidimensional maps, IEEE Transactions on Neural Networks 3 (5) (1992).